Journal of Catalysis 268 (2009) 260–267

Contents lists available at ScienceDirect

Journal of Catalysis

journal homepage: www.elsevier.com/locate/jcat

Catalytic dehydration of glycerol over vanadium phosphate oxides in the presence of molecular oxygen

Feng Wang [a,*], Jean-Luc Dubois [b], Wataru Ueda [a,*]

[a] Catalysis Research Center, Hokkaido University, North 21, West 10, Sapporo 001-0021, Japan
[b] Arkema France, 420 Rue d'Estienne d'Orves, 92705 Colombes, France

ARTICLE INFO

Article history:
Received 7 August 2009
Revised 25 September 2009
Accepted 25 September 2009
Available online 24 October 2009

Keywords:
Dehydration
Glycerol
Acrolein
Acetaldehyde
Hemihydrate vanadium phosphate oxide
Molecular oxygen

ABSTRACT

We report the dehydration of glycerol over vanadium phosphate oxide (VPO) catalysts. Catalytic reactions were conducted in a gas-phase fixed-bed reactor at temperatures from 250 to 350 °C with O_2/glycerol ratios of 0–13.6. Hemihydrate $VOHPO_4{\cdot}0.5H_2O$ oxide emerged as the best catalyst. At 300 °C, glycerol conversion was 100% with 66% selectivity to acrolein and 14% selectivity to acetaldehyde. The carbon balance was 93%. The advantage of adding oxygen is that the catalyst can be maintained in an oxidized state. It was shown that carbon deposition was inhibited and that side products were greatly reduced. Moreover, the structure of the catalyst did not change during the reaction as confirmed by X-ray diffraction (XRD), infrared (IR), and thermogravimetric–differential thermal analysis (TG–DTA). We also investigated the reaction network and proposed a possible reaction pathway.

1. Introduction

Glycerol is the main by-product of transesterification of vegetable oils (triglycerides) and methanol for producing biodiesel. In this process, 1000 kg of biodiesel usually generates about 100 kg of glycerol. Increase in biodiesel production therefore results in the accumulation of glycerol. Currently, about 350,000 tons of glycerol is produced per annum in the USA and about 600,000 tons is produced per annum in Europe. The levels will increase because of the implementation of EU directive 2003/30/EC, which requires replacement of 5.75% of petroleum fuels with biofuel across all member states by 2010. Therefore, it is imperative to find value-added ways of utilizing glycerol that will be beneficial for both the environment and biodiesel manufacturing. In recent years, the use of glycerol has become an important research topic in catalysis. Several reviews have recently been published giving a comprehensive overview of the topic [1–3].

Glycerol has been converted to mono, di, and triacetylesters by acetylation reaction or to glycerol carbonate by carboxylation reaction with CO_2 or urea [4,5]. There are some reports on the synthesis of 1,3-propanediol either by direct hydrogenation or by processes of fermentation and on the synthesis of epichlorohydrine and polyethers [6]. Catalytic hydrogenation of glycerol has been reported to produce 1,2-propanediol, ethylene glycol, and propane over Pt, Pd, Ru, Ni, and Co catalysts [7–10]. There have been several studies on the decomposition of glycerol to syngas by pyrolysis reaction or to hydrogen by reforming reaction [11–13]. In some cases, glycerol is considered as "organic water" and employed as a solvent [14,15]. Selective oxidation of glycerol to acids has been conducted over precious metal catalysts in liquid-phase with oxygen or hydrogen peroxide as an oxidant to produce highly functionalized carboxylic acids, such as tartronic acid, glyceric acid, hydroxypyruvic acid, and glyoxylic acid [16–18].

Acrolein is an important product from glycerol dehydration. In 1933, Scheering–Kahlbaum reported glycerol dehydration over pumice-supporting lithium phosphate or copper phosphate catalysts at temperature from 300 to 600 °C [19]. Several groups, such as Corma et al. [20], Xu et al. [21–23], and Tsukuda et al. [24] have recently studied glycerol dehydration over acid catalysts, such as sulfates, phosphates, zeolites, and metal oxides, under conditions of gas-phase, liquid-phase, supercritical water, or hot-compressed water conditions [25–29]. These studies had various problems such as harsh reaction conditions, severe coke formation, and large amounts of by-products. These problems must be solved in order to achieve continuous and economical industrial production. Arkema Company described a way in patents to inhibit catalyst deactivation and reduce side products through addition of oxygen during the dehydration reaction [30,31]. Preferred catalysts described in these patents are acidic materials, such as WO_3, ZrO_2, ZrO_2/SO_4, and Al_2O_3.

* Corresponding authors. Fax: +81 11 706 9164 (F. Wang).
E-mail addresses: wangfeng@cat.hokudai.ac.jp (F. Wang), ueda@cat.hokudai.ac.jp (W. Ueda).

0021-9517/$ - see front matter © 2009 Elsevier Inc. All rights reserved.
doi:10.1016/j.jcat.2009.09.024

The objective of this study was to develop a process with high selectivity for acrolein and without severe coke formation. We focused on glycerol dehydration in the presence of oxygen over VPO catalysts. The advantages of adding oxygen in the dehydration reaction are as follows. First, an oxidative atmosphere for dehydration reaction is effective for inhibiting or reducing carbon deposition and thus for increasing longevity of the catalyst. Strongly adsorbed hydrocarbon species on the catalyst surface can be quickly removed by oxidation before the formation of intensive carbon coke, and catalytic active sites are recovered. Second, glycerol is a strong reductant at a high reaction temperature. The presence of oxygen enables maintenance of the catalytic redox cycle of metal oxides. For example, the reduction of metal centers with higher valences, such as V^{5+} to V^{4+} or V^{3+}, usually leads to catalyst deactivation. Third, it would be interesting if conversion of glycerol to acrylic acid is realized in one-step. Tandem-type reactors, one reactor being loaded with a dehydration catalyst to produce acrolein and the other reactor being loaded with an oxidation catalyst to produce acrylic acid, are applicable in industrial process. However, a one-step process would greatly reduce the investment cost and simplify the engineering process. Furthermore, a better heat balance over the catalyst bed could be achieved by a one-step process because the dehydration reaction is endothermic and the oxidation is exothermic.

VPO oxides, such as pyrophosphate $(VO)_2P_2O_7$, have been studied in the selective oxidation of butane, isobutene, propane, or ethane to the corresponding acids [32–37]. As far as we know, VPO oxides have not been studied for the utilization of glycerol. We report here glycerol dehydration over VPO oxides in the presence of molecular oxygen. We found that vanadyl hydrogen phosphate hemihydrate $VOHPO_4{\cdot}0.5H_2O$ exhibited the best performance with 66% selectivity for acrolein at 100% conversion of glycerol and without coke deposition. Its catalytic performance is comparable with that in the literature works. The carbon balance was 93%, which was the highest among the three catalysts and was even better than the previously reported results. Furthermore it is the first time that $VOHPO_4{\cdot}0.5H_2O$ is reported as an active and selective catalyst. The stability of the catalyst was examined and the possible reaction pathways were investigated.

2. Experimental

2.1. Preparation of catalysts

All reagents were of analytical-reagent grade purchased from Wako Pure Chemical Company and were used without further purification. Distilled water prepared by using a Yamato Autostill WG25 (Tokyo, Japan) was utilized throughout this work.

The preparation of dihydrate $VOPO_4{\cdot}2H_2O$ has been reported elsewhere [38]. In brief, a mixture of V_2O_5 (24 g), H_3PO_4 (85%, 133 mL), and H_2O (577 mL) was refluxed at 115 °C for 16 h. The reaction produced a bright-yellow solid, which was collected by filtration, washed with 100 mL acetone, and dried for 10 h under ambient conditions. Both XRD and IR characterizations confirmed the solid to be $VOPO_4{\cdot}2H_2O$. $VOHPO_4{\cdot}0.5H_2O$ was prepared by reduction of $VOPO_4{\cdot}2H_2O$ in organic alcohol. A suspension of $VOPO_4{\cdot}2H_2O$ (5 g) powder in 2-butanol (50 mL) was stirred under reflux for 23 h (oil bath temperature: 101 °C). The resulting light-blue solid was collected by filtration, washed with 100 mL of acetone, and dried for 10 h under ambient conditions. The solid was characterized by XRD and IR and its phase was confirmed to be hemihydrate $VOHPO_4{\cdot}0.5H_2O$. The precursor of $VOHPO_4{\cdot}0.5H_2O$ (1.0 g) was treated at 550 °C for 4 h under nitrogen (50 mL min^{-1}) at the heating rate of 1 °C min^{-1}. The resulting gray solid was confirmed to be pyrophosphate $(VO)_2P_2O_7$ by XRD and IR.

2.2. Characterization of catalysts

XRD measurements were performed with a Rigaku RINT Ultima+ diffractometer with Cu Kα radiation (Kα 1.54056 Å) and X-ray power of 40 kV/20 mA. Field emission scanning electron microscopy (FE-SEM) was performed on a JSM-7400F (JEOL). The samples for SEM were dusted on an adhesive conductive carbon paper attached to a brass mount. Specific surface areas were measured by nitrogen adsorption at 77 K using the Brunauer–Emmett–Teller (BET) method over Autosorb 6AG (Quantachrome Instruments). IR spectra were recorded on a Perkin–Elmer FT-IR spectrometer by accumulating 32 scans at a spectrum resolution of 2 cm^{-1}. The sample pellet of 1.5 mm in diameter was prepared by pressing a mixture of the sample and KBr. TG–DTA measurements were performed in a TG-8120 (Rigaku) thermogravimetric analyzer. Dry air provided by a pressured tank with a flow rate of 30 mL min^{-1} was used as the carrier. The baseline was subtracted from a blank run. Catalyst and reference alumina samples were loaded into twin holders. The experiments were carried out from room temperature to 700 °C with a heating rate of 10 °C min^{-1}.

2.3. Catalytic tests

Glycerol dehydration tests were conducted under normal pressure in a vertical fix-bed homemade Pyrex reactor with internal diameter of 5 mm. The catalyst was mixed with quartz (50–70 mesh) and loaded in the middle of the reactor with quartz wool packed in both ends. The catalyst was pretreated at 300 °C for 1 h in a flow of nitrogen (18 mL min^{-1}). The reaction temperature was monitored by a thermocouple inserted into the middle of the catalyst. Typically, 0.2 g of catalyst was used and diluted with 3.0 g of quartz. Aqueous glycerol (20% wt/wt) was fed at the speed of 0.50 g h^{-1} by a syringe pump. The composition of fed gas was N_2:O_2:H_2O:glycerol, equal to 57.2:12.7:28.7:1.4 in molar ratio. The sampling interval was 10 h. The product was collected in a cold trap (−78 °C, mixture of acetone and dry ice). The collected product was dissolved in 5 mL of aqueous solution of internal standard 2-butanol and was analyzed by GC–MS (Shimadzu 15A) with a capillary column (GL Sciences, TC-FFAP 60 m × 0.25 mm × 0.5 μm) and a flame ionization detector (FID). The chromatograph column was run at 110–250 °C with a ramping rate of 5 °C min^{-1} and at 250 °C for 10 min. Volatile compounds running out of the cold trap were analyzed by three online GCs with two thermal conductivity detectors (TCD) and one FID detector. The GC analyses allowed quantifications of CO, CO_2, acetaldehyde, acrolein, and acetic acid.

All the results of GC analyses for liquid-phase and gas-phase were combined to calculate the conversion, product selectivity, and mass balance. Calculation of glycerol conversion (X_{gly}, mol%) was based on the concentrations of glycerol at the inlet and the outlet of the reactor:

$$X_{gly} = \frac{M_{gly,in} - M_{gly,out}}{M_{gly,in}} \times 100, \quad (1)$$

where $M_{gly,in}$ and $M_{gly,out}$ are the quantities of fed and unreacted glycerol, respectively. The conversion of oxygen (X_{oxy}, mol%) was determined using online GC by measuring the integration area ratios of oxygen to nitrogen for the inlet and outlet gases, assuming that the amount of nitrogen was constant. Product selectivity (S_i, mol%) was calculated from the molar concentrations of product and glycerol according to Eq. (2):

$$S_i = \frac{M_i}{M_{gly,in} - M_{gly,out}} \times \frac{z_i}{3} \times 100, \quad (2)$$

where z represents the number of carbon atoms, for example, $z = 3$ for glycerol and M_i represents the detected molar quantity of

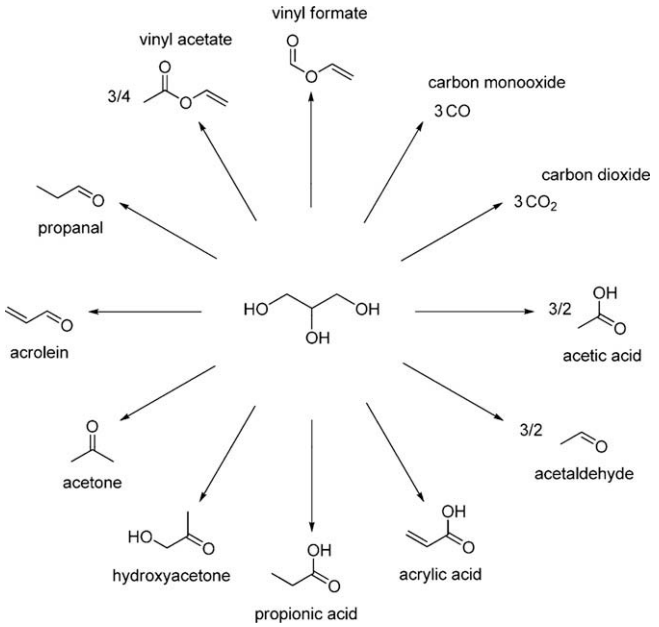

Fig. 1. The equations and products for calculating carbon balance.

product *i*. Carbon balance (mol%) was calculated by summing up the unreacted glycerol and the total quantities of detected and calibrated products, as shown in Fig. 1.

3. Results and discussion

3.1. Characterization of the catalysts

Three VPO materials, dihydrate ($VOPO_4{\cdot}2H_2O$), hemihydrate ($VOHPO_4{\cdot}0.5H_2O$), and pyrophosphate ($(VO)_2P_2O_7$), were prepared. Their XRD patterns are shown in Fig. 2. The reflection peaks at $2\theta = 12.1°$, 18.7°, 24.1°, and 29.0° are indexed to be (0 0 1), (1 0 1), (0 0 2), and (2 0 0) plane of lamellar $VOPO_4{\cdot}2H_2O$ phase, respectively. After reduction in 2-butanol, a strong reflection peak appears at $2\theta = 15.8°$, which corresponds to the (0 0 1) plane of $VOHPO_4{\cdot}0.5H_2O$ phase. During the reduction process, 2-butanol is oxidized and $VOPO_4{\cdot}2H_2O$ phase is reduced, resulting in the intercalation of hydrogen into crystalline layers. Under thermal treatment in nitrogen atmosphere, the $VOHPO_4{\cdot}0.5H_2O$ phase undergoes a topotactic dehydration to $(VO)_2P_2O_7$ phase, as confirmed by the characteristic peaks at $2\theta = 23.3°$, 28.7°, 30.3°, and 43.6°, which are in good agreement with those in the literature [32,39].

In FT-IR spectra (Fig. 3), intensive changes are observed in the range of 400–2000 cm^{-1}. Bending modes of water molecules can be seen around 1630 cm^{-1} in three samples. In general, bands between 600 and 1300 cm^{-1} correspond to the stretching of P–O and V–O, while bands below 600 cm^{-1} are assigned to the bending of O–V–O and O–P–O [40]. The IR spectrum shows 1084 cm^{-1} (ν_{as} (P–O)), 994 cm^{-1} (ν (V=O)), 944 cm^{-1} (ν (V–OH)), 672 cm^{-1} (δ (V–OH) or δ (P–OH)), and 576 cm^{-1} (δ_{as} P–O–P) bands, which are characteristics of $VOPO_4{\cdot}2H_2O$ [41]. IR bands of 1200 cm^{-1} (ν_{as} (PO_3)), 1132 cm^{-1} (δ_{ip} (P–OH)), 1104 cm^{-1} (ν_{as} (PO_3)), 1054 cm^{-1} (ν_{as} (PO_3)), 980 cm^{-1} (ν (V=O)), 931 cm^{-1} (ν (P–OH)), 684 cm^{-1} (ω (coordinated H_2O)), 642 cm^{-1} (δ_{oop} (P–OH)), 548 cm^{-1} (δ (OPO)), 534 cm^{-1} (δ (OPO)), 480 cm^{-1} (δ (OPO)), and 417 cm^{-1} (δ (OPO)) are characteristics of $VOHPO_4{\cdot}0.5H_2O$ [40]. IR bands occurring at 1244 cm^{-1} (ν_{as} (PO_3)), 1220 cm^{-1} (δ_{ip} (P–OH)), 1142 cm^{-1} (ν_{as} (PO_3)), 1084 cm^{-1} (ν_{as} (PO_3)), 970 cm^{-1} (ν (V=O)), 744 cm^{-1} (ν_s (P–O–P)), 634 cm^{-1} (ν_{as} (PO_3)), 576 cm^{-1} (δ (OPO)), 514 cm^{-1} (δ (PO_3)), and 456 cm^{-1} (δ (OPO)) belong to the phase of $(VO)_2P_2O_7$ [42].

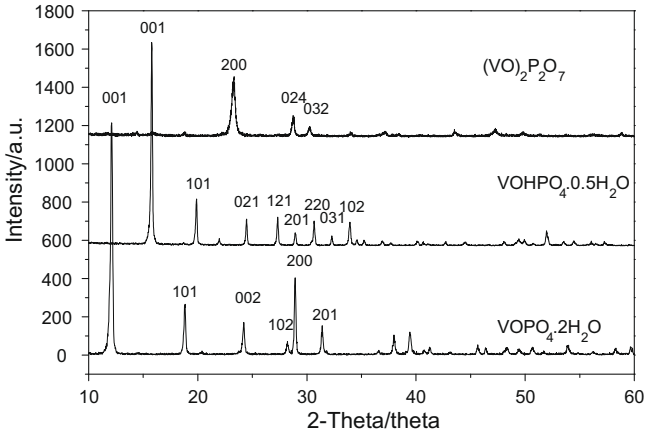

Fig. 2. XRD patterns of $VOPO_4{\cdot}2H_2O$, $VOHPO_4{\cdot}0.5H_2O$, and $(VO)_2P_2O_7$.

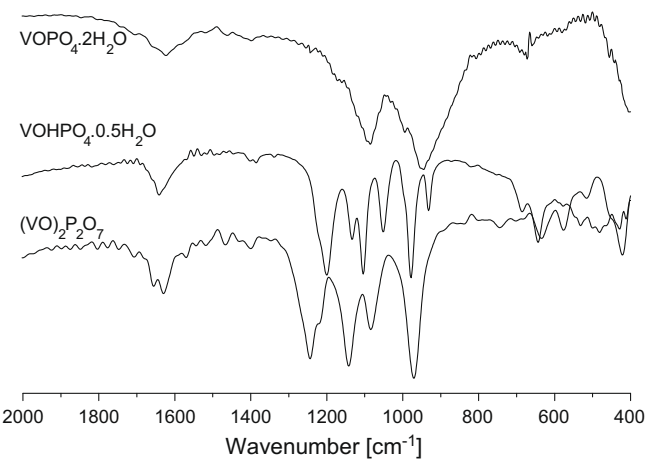

Fig. 3. FT–IR spectra of $VOPO_4{\cdot}2H_2O$, $VOHPO_4{\cdot}0.5H_2O$, and $(VO)_2P_2O_7$.

Representative SEM images are shown in Fig. 4. The three samples have platelet morphologies with uniform particle size distribution. $VOPO_4{\cdot}2H_2O$ mainly consists of crystals with sizes of 2–4 μm and thicknesses of 0.1–0.2 μm. The reduction of $VOPO_4{\cdot}2H_2O$ produces $VOHPO_4{\cdot}0.5H_2O$ orienting along the (0 0 1) plane, which has larger platelets with sizes of 10–20 μm and thicknesses of 0.1–0.3 μm. The surface of the $(VO)_2P_2O_7$ platelet is covered with pores owing to the dehydration reaction. The specific surface areas of $VOPO_4{\cdot}2H_2O$, $VOHPO_4{\cdot}0.5H_2O$, and $(VO)_2P_2O_7$ are 7 $m^2\ g^{-1}$, 12 $m^2\ g^{-1}$, and 8 $m^2\ g^{-1}$, respectively, which agree well with the reported results [39,43].

3.2. Screening catalysts

Catalytic results over the three VPO catalysts in the presence of molecular oxygen are shown in Table 1. The major products of the glycerol dehydration were acrolein, acetaldehyde, acetic acid, acrylic acid, propionic acid, and esters. Products grouped under the label of "other CHO" include methyl vinyl ketone, butanone, cyclopentanone, and methacrolein. We did not observe the formation of CO, probably because of the oxygen-rich reaction condition. In most cases, carbon balance was less than 100%. Several factors may contribute to the difference, such as some unknown minor peaks in chromatograms, some decomposed products during analysis in the GC injector, and a small amount of carbon deposits. The

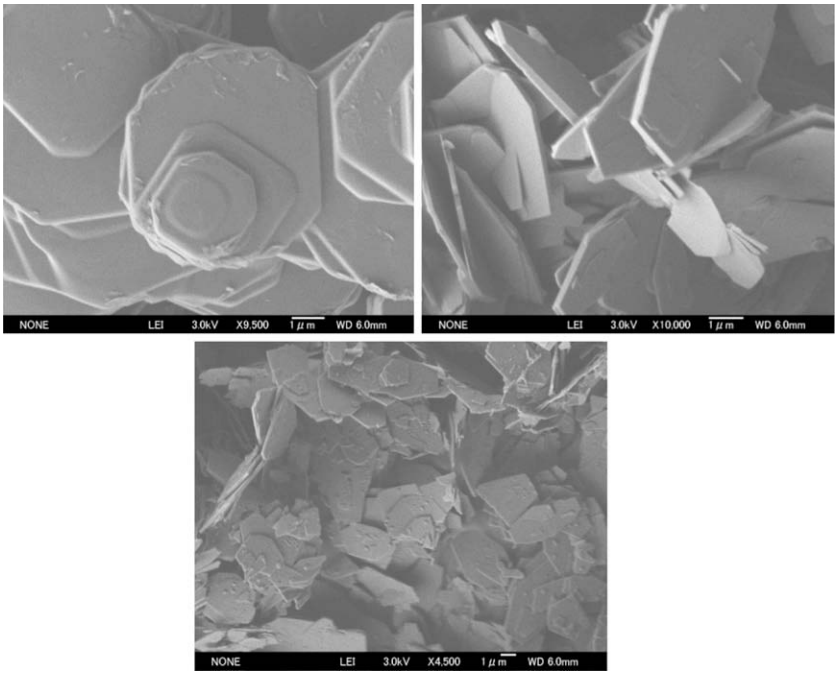

Fig. 4. SEM images of $VOPO_4{\cdot}2H_2O$ (upper left), $VOHPO_4{\cdot}0.5H_2O$ (upper right), and $(VO)_2P_2O_7$.

Table 1
Catalytic results over the three VPO catalysts.

Catalyst	$VOPO_4{\cdot}2H_2O$	$VOHPO_4{\cdot}0.5H_2O$	$(VO)_2P_2O_7$
Glycerol conversion (mol%)	81.0	100	100
Oxygen conversion (mol%)	14	14	7
Carbon balance (mol%)	85	93	72
Products distribution (mol%)			
Acrolein	55	66	41
Acetaldehyde	12	14	4
Hydroxyacetone	0	4	12
Acetone	0	0.2	0
Propanal	0	0.4	0.1
Acetic acid	0	5	1
Acrylic acid	1	3	1
Esters	0	2	0
CO_2	6	0.5	1
Other CHO	16	4	14

Reaction conditions: 0.2 g of catalyst was used and diluted with 3.0 g of quartz. The aqueous glycerol (20% wt/wt) was fed at the speed of 0.5 g h^{-1} by a syringe pump. The composition of fed gas was N_2:O_2:H_2O:glycerol, equal to 57.2:12.7:28.7:1.4 in mole ratio. The sampling interval was 10 h.

conversion of oxygen (C_{oxy}) is 6–14%. This value is larger than the calculated value by summing up the total quantity of oxygen sources from products, such as acetic acid, acrylic acid, CO, and CO_2. There are two possible reasons for the missing oxygen: (1) water as a co-feeding substance was not included in the calculation and (2) some unknown by-products probably contributing to oxygen consumption were not determined.

$VOHPO_4{\cdot}0.5H_2O$ is often used as a precursor of $(VO)_2P_2O_7$ catalyst. However, catalysis by $VOHPO_4{\cdot}0.5H_2O$ has been overlooked. In this study, we found that $VOHPO_4{\cdot}0.5H_2O$ is the best catalyst, offering 100% conversion of glycerol, 66% selectivity to acrolein, 14% selectivity to acetaldehyde, and 5% selectivity to acetic acid. Its catalytic performance is comparable with that in the literature works. The carbon balance was 93%, which is the highest among the three catalysts and is even better than the literature results. We employed the $VOHPO_4{\cdot}0.5H_2O$ catalyst in detailed studies.

The reaction produced substantial amounts of CO_2, CHO, and unknown products (total selectivity of ca. 25%) over the $VOPO_4{\cdot}2H_2O$ catalyst. Pyrophosphate $(VO)_2P_2O_7$ catalyst, which is well known in butane oxidation, realized 100% conversion of glycerol but produced 41% selectivity to acrolein with more than 25% selectivity to by-products. The carbon balance of 72% was much smaller than that of the reaction over the $VOHPO_4{\cdot}0.5H_2O$. We speculate that $(VO)_2P_2O_7$ catalyst strongly adsorbs glycerol, acrolein, and other reaction intermediates. The strong adsorption sites, usually acid sites, are generated by thermal treatment of $VOHPO_4{\cdot}0.5H_2O$ at a high temperature. Moreover, the 12% selectivity to hydroxyacetone over the $(VO)_2P_2O_7$ catalyst is more than those over the other two catalysts, suggesting that the catalyst is active for dehydration reaction at a terminal hydroxyl group of glycerol.

Although the dehydration of glycerol was conducted in oxygen atmosphere, we did not observe high selectivity to acrylic acid. There have been some reports of oxidation of acrolein over Mo, V, or W oxides [44,45]. Arkema described in a patent that a small amount of acrylic acid was formed in a single step from glycerol over MoVWO-type catalysts [46]. In the present study, however, although excess oxygen to glycerol (oxygen:glycerol = 9.1:1) was added, acrolein was not oxidized to acrylic acid. The selectivities for acrylic acid were less than 5% over the three catalysts. This result indicates that the VPO catalysts are capable of catalyzing the dehydration of glycerol to acrolein but are unable to catalyze the oxidation of acrolein to acrylic acid. The presence of oxygen inhibited the formation of hydrogenated products such as propane, butane, and diols reported in the dehydration of glycerol without adding oxygen [20]. The effect of oxygen concentration will be discussed in the following section.

3.3. Effect of oxygen concentration

The concentration of oxygen in the feeding stream had a remarkable effect on the catalytic results of glycerol dehydration as shown in Table 2. The $VOHPO_4{\cdot}0.5H_2O$ catalyst was inactive in the absence of oxygen with 43% conversion of glycerol and carbon balance of 68%. When oxygen was co-fed with glycerol in a ratio of

Table 2
Effect of oxygen concentration on catalytic results over the $VOHPO_4{\cdot}0.5H_2O$ catalyst.

O_2/N_2 (mL/mL)	0/18	0.5/18	2/18	4/18	6/18
Ratio of O_2/glycerol (mol/mol)	0	1.1	4.5	9.1	13.6
Glycerol conversion (mol%)	43	90	95	100	100
Oxygen conversion (mol%)	0	79	40	14	15
Carbon balance (mol%)	68	66	77	91	81
Products distribution (mol%)					
Acrolein	35	24	51	66	43
Acetaldehyde	6	4	15	15	15
Hydroxyacetone	33	15	3	4	0
Acetone	0	0	0	0	0
Propanal	0	0	0	0	0
Acetic acid	0	4	4	5	25
Acrylic acid	0	2	2	3	8
CO_2	0	2	5	1	7
Other CHO	1	15	5	4	1

Reaction conditions: see note in Table 1.

1.1 (oxygen:glycerol), the conversion of glycerol significantly increased to 90% with better carbon balance. Further increase in oxygen concentration increased the conversion of glycerol, decreased the unknown products, and improved the carbon balance. One hundred percent conversion of glycerol was achieved at the oxygen/glycerol ratio of 9.1. Increase in oxygen/glycerol ratio up to 13.6 did not change the conversion of glycerol. A blank test (without a catalyst) showed that there was no autocatalysis or catalysis initiated by reactor walls. Therefore, the observed conversion of glycerol truly took place on the catalyst.

Catalytic active sites easily get blocked and poisoned by strongly adsorbed substances, such as heavy carbon species, finally deactivating the catalyst. We washed a used catalyst from a reaction without adding oxygen with dimethyl sulfoxide solvent. The catalyst was filtered out and the filtrate was analyzed by GC–MS. We found a large amount of mass fragments with m/z ratios in the range of 200–500. These fragments indicate that heavy carbon species had formed on the catalyst surface [47]. On the other hand, we observed only a small amount of those fragments when treating the catalyst from a reaction conducted with oxygen/glycerol ratio of 9.1 in a similar way. TG–DTA results of used catalysts are shown in Fig. 5. The catalyst of the reaction without adding oxygen has a weight loss at 600 °C in the TG curve and an exothermal peak in the DTA curve correspondingly, ascribed to the combustion of carbon species. However, similar weight loss and exothermal peak

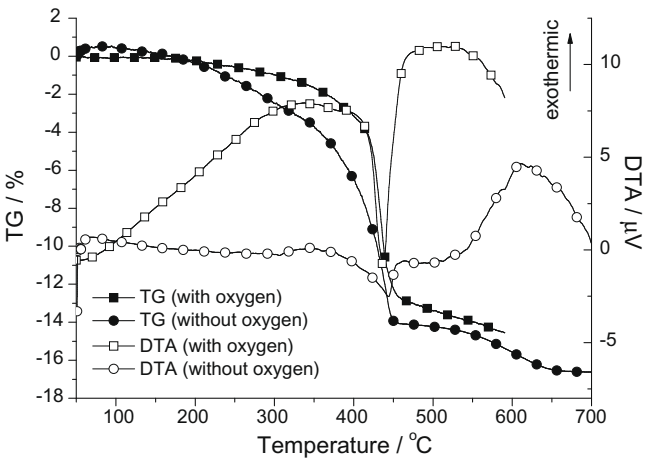

Fig. 5. Comparison of TG–DTA profiles of the used catalyst from a reaction without the addition of oxygen and the used catalyst from a reaction with an O_2/glycerol ratio of 9.1.

did not appear on the used catalyst of the reaction with oxygen. Thus, the presence of oxygen can greatly decrease the adsorbed carbon species. Such species are converted into heavy carbon species, such as carbon coke, in a long-run reaction. Carbon coke is relatively stable and requires a higher temperature to be removed than in situ oxidation removal as soon as it is formed. Moreover, oxygen can maintain the redox cycle of metal sites. During the reaction, the catalyst surface contains many species with C–O, C=O, C–C, C=C, or C–H bonds. Conversion of these species usually needs oxygen species, and thus the catalyst surface easily gets starved for oxygen. Once oxygen is removed from the catalyst surface, an acid site will be created, which in turn serves as an active site for removal of next oxygen. Therefore, timely supply of oxygen is necessary to keep the catalyst active. In this study, we added excess oxygen to avoid reduction of the catalyst, a method similar to butane oxidation, where excess oxygen is employed to avoid over-reduction of the catalyst [36].

The selectivity to hydroxyacetone decreased with increasing oxygen concentration. The selectivity to hydroxyacetone was 33% without addition of oxygen, rapidly decreased to 15% with addition of oxygen (oxygen/glycerol = 1.1), and became 0% with further addition of oxygen (oxygen/glycerol = 13.6). Hydroxyacetone is the product of 1,2-dehydration with loss of the hydroxyl group from the terminal carbon [48]. Calculations show that 1,2-dehydration resulting in the loss of the central or terminal hydroxyl group has nearly equal energy barriers (terminal: 73.2 kcal mol^{-1}; central: 70.9 kcal mol^{-1}) [48]. In this study, the change in hydroxyacetone selectivity may have depended on the nature of the active sites, which can be modified in situ by molecular oxygen. It is also possible that hydroxyacetone is oxidized to other products with increasing oxygen concentration, such as methylglyoxal, which is difficult to be determined in the present analysis.

The selectivities to acrolein and acetaldehyde increased with the increase in oxygen concentration until the oxygen/glycerol ratio reached 9.1, suggesting that oxygen promotes 1,2-dehydration with the loss of the hydroxyl group from the central carbon, and 1,3-dehydration route, through which acetaldehyde is formed [48]. Further increase in the oxygen/glycerol ratio from 9.1 to 13.6 decreased the selectivity of acrolein from 66% to 43%, slightly affected the selectivity of acetaldehyde, and enhanced the selectivity of acetic acid from 5% to 25% and that of CO_2 from 0.5% to 7%. Acetic acid and CO_2 are the products of acrolein oxidation since only the selectivity to acrolein sharply decreased. In the presence of oxygen, the reaction realizes good carbon balance and produces fewer by-products. Corma et al. [20] and Chai et al. [21–23] reported catalytic conversion of aqueous glycerol solution without oxygen over acid-type catalysts. In their studies, large amounts of coke formation (3–30%) were observed. Even under similar reaction conditions without adding oxygen, the present study showed that $VOHPO_4{\cdot}0.5H_2O$ is a better catalyst for converting glycerol to acrolein in high selectivity while maintaining high activity and generating less coke formation and fewer by-products.

3.4. Effect of reaction temperature

The conversion of glycerol and the conversion of oxygen remarkably increased with increase in reaction temperature from 250 °C to 350 °C (Table 3). The selectivities to acrolein and hydroxyacetone increased simultaneously. At 350 °C, C–C bond breakage took place as indicated by the generation of large amounts of C1 and C2 products. The selectivity to hydroxyacetone decreased from 29% at 250 °C to 0% at 350 °C, suggesting that 1,2-dehydration at a lower temperature mainly occurs at the central carbon site. The selectivity to acrylic acid was 8% at 350 °C, indicating that a high temperature is favorable for oxidizing acrolein to acrylic acid. Reaction temperature of 300 °C is suitable for achieving high

Table 3
Effect of reaction temperature on catalytic results over the $VOHPO_4{\cdot}0.5H_2O$ catalyst.

Temperature (°C)	250	275	300	325	350
Glycerol conversion (mol%)	68	78	100	100	100
Oxygen conversion (mol%)	0	10	14	30	27
Carbon balance (mol%)	70	74	91	80	74
Products distribution (mol%)					
Acrolein	12	25	66	48	36
Acetaldehyde	2	5	15	18	20
Hydroxyacetone	29	14	4	0	0
Acetone	0	7	0	0	0
Propanal	0	0	0	0	0
Acetic acid	9	3	5	18	15
Acrylic acid	0	1	3	5	8
CO	0	0	0	6	14
CO_2	0	2	1	5	8
Other CHO	7	14	4	0	0

Reaction conditions: see note in Table 1.

selectivity to acrolein and carbon balance larger than 90%. Compared with the temperatures of 300–700 °C for conducting reactions in previous works, the present reaction temperature is mild.

3.5. Effect of space velocity rate

Change in the space velocity rate (WHSV) is realized by adjusting the weight of the catalyst and keeping the feeding gas constant (Table 4). The space velocity rate has little effect on product distributions. The main products were acrolein and acetaldehyde. With increase in WHSV from 2.6 to 20.5 h^{-1}, the conversion of oxygen decreased. The conversion of glycerol was 100% even when the reaction is performed at a high space velocity rate (20.5 h^{-1}), indicating that the $VOHPO_4{\cdot}0.5H_2O$ catalyst is highly reactive for glycerol dehydration.

3.6. Stability of the $VOHPO_4{\cdot}0.5H_2O$ catalyst

We used several techniques to study the stability of the $VOHPO_4{\cdot}0.5H_2O$ catalyst. We previously thought that the $VOHPO_4{\cdot}0.5H_2O$ was unstable and perhaps changed to other active phases, catalyzing the reaction. However, the used catalyst showed an IR spectrum similar to that of a fresh one as shown in Fig. 6. A small increase in IR transmission intensity appears at 1620 cm^{-1}, which is assigned to the vibration of water, suggesting that the used catalyst contains more water. TG–DTA analysis (Fig. 7) revealed that the two catalysts have similar weight loss and thermal transformation except that (1) the central decomposition temperature of the used catalyst is 434 °C, which is 6 °C lower than that (440 °C) of the fresh catalyst and (2) there was greater weight loss for the used catalyst at temperatures between 400 °C and 500 °C. The former difference is explained by the disturbance of crystalline disorder by water absorption, and the latter is caused by slow structure dehydration. Globally, the used catalyst has a weight loss of 10.2%, and the fresh one has a weight loss of 9.5%. XRD characterizations (Fig. 8) showed that the two catalysts have nearly identical structures except that the *d* spacing of the (0 0 1) facet of the used catalyst is slightly shifted to a lower angle, implying widening of the two adjacent [0 0 *l*] layers. Such an effect is probably caused by partial hydration of the V=O or P=O bond between the two adjacent layers. Based on IR and TGA results, it is concluded that the $VOHPO_4{\cdot}0.5H_2O$ catalyst is stable during the reaction. Small changes take place because of water adsorption since the reaction is conducted under humid reaction conditions (partial water pressure: 0.0287 MPa).

Table 4
Effect of space velocity rate (WHSV) on catalytic results over the $VOHPO_4{\cdot}0.5H_2O$ catalyst.

WHSV (h^{-1})	20.5	10.2	5.1	2.6
Glycerol conversion (mol%)	100	100	100	100
Oxygen conversion (mol%)	11	14	28	32
Carbon balance (mol%)	86	91	86	85
Products distribution (mol%)				
Acrolein	65	66	62	62
Acetaldehyde	18	15	14	17
Hydroxyacetone	0	4	0	0
Acetone	0	0	0	0
Propanal	0	0	0	0
Acetic acid	5	5	10	5
Acrylic acid	4	3	6	4
CO_2	2	1	3	7
Other CHO	2	4	1	2

Reaction conditions: see note in Table 1.

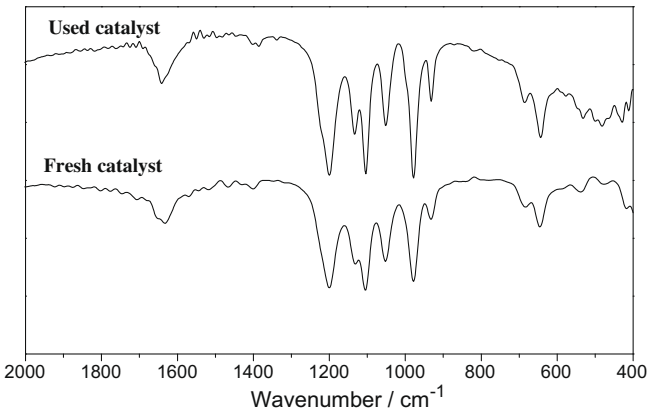

Fig. 6. IR spectra of used and fresh $VOHPO_4{\cdot}0.5H_2O$ catalyst. The used catalyst was collected after removing the quartz diluents by sieving, and used without any treatment.

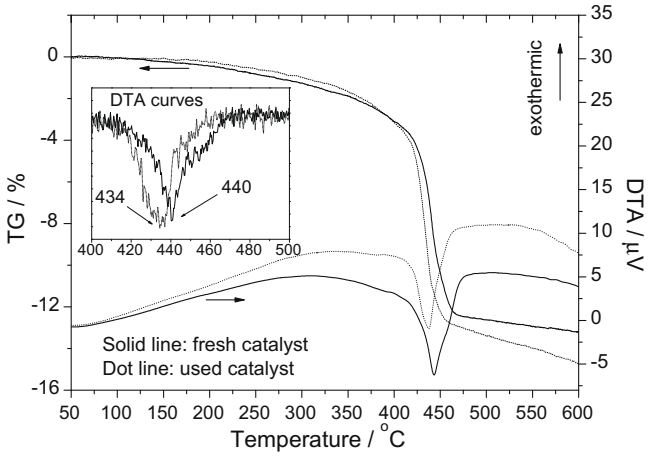

Fig. 7. TG–DTA curves of the used and fresh $VOHPO_4{\cdot}0.5H_2O$ catalyst.

3.7. Reaction pathway

The complexities of the dehydration of glycerol in the presence of oxygen are largely because of the three hydroxyl groups and highly functionalized derivatives. To classify the reaction pathways, we employed several major products as substrates to investigate their products under the same reaction conditions: reaction

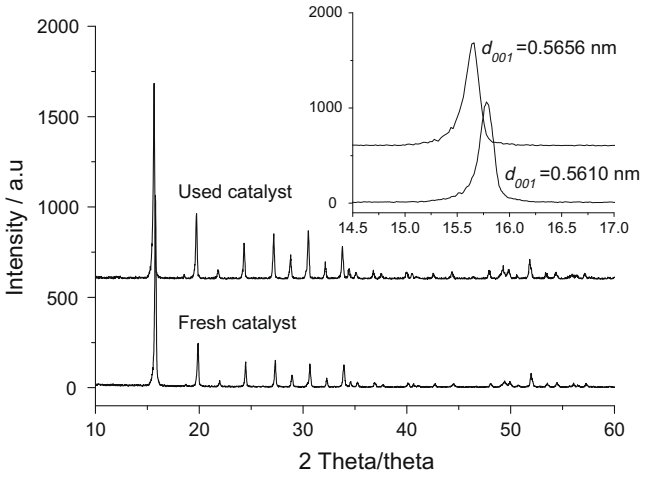

Fig. 8. XRD patterns of the used and fresh $VOHPO_4{\cdot}0.5H_2O$ catalyst.

temperature of 300 °C, 0.1 MPa, and 0.2 g of catalyst diluted by 3.0 g of quartz. Catalytic results are given in Fig. 9.

Acetaldehyde conversion: Twenty percent conversion of acetaldehyde was obtained with 100% selectivity to acetic acid. It was proposed by Corma et al. that acetaldehyde also further reacted to form oligomers [20]. However, we did not observe the formation of oligomers, owing to the oxidative atmosphere.

Hydroxyacetone conversion: The conversion of hydroxyacetone was 55%, which is far less than that of glycerol, suggesting that hydroxyacetone is less active than glycerol. The products were acetone (35%), acetic acid (28%), and acetaldehyde (21%). The formation of acetone revealed that some step may involve the hydrogenation of 1,2-propanediol, an unstable intermediate that was not detected in this study [48]. Surface hydroxyl and adsorbed hydrocarbon species possibly provide hydrogen species for hydrogenation. The formation of acetaldehyde may be via 2-oxopropanal, an active intermediate formed by the dehydrogenation or oxidation of hydroxyacetone [49]. Another missing carbon may be converted to CO or adsorbed carbon species. Acetic acid is probably generated from the oxidation of acetaldehyde. In the test, we did not observe the product of acrolein. This result suggests that the dehydration of glycerol occurs in two distinct ways, one leading to hydroxyacetone and the other leading to acrolein.

Acetone conversion: The conversion of acetone was 10%, indicating that acetone was less active than acetaldehyde and hydroxyacetone, largely owing to its robust molecular structure. The major product was acetic acid with 80% selectivity. Oxidation of acetone needed breakage of either the C–C bond or the C–H bond. We did not observe an oxidized product via C–H bond activation at the terminal carbon site of acetone, and we detected acetic acid and acetaldehyde, formed by C–C bond activation. As shown by Corma et al., acetone could be converted into butene and acetic acid via a bimolecular mechanism [20]. We did not obtain a butane product in this study.

Acrolein conversion: The conversion of acrolein was only 4% with acetaldehyde, acrylic acid, acetic acid, and propanal as main products, indicating that acrolein is much less reactive than hydroxyacetone, acetaldehyde, and acetone. Although the reaction was conducted in the presence of excess oxygen, it was still difficult for acrolein to be oxidized. The test confirmed that the $VOHPO_4{\cdot}0.5H_2O$ catalyst has limited oxidation ability. Since 20% conversion of acetaldehyde (C2) was achieved under the same reaction conditions, we suggest that a steric effect or geometric adsorption may play a key role, that is, a short molecule (C2) is easier to be oxidized than a longer molecule (C3).

Acrylic acid and acetic acid conversion: We are surprised that both acrylic acid and acetic acid are inactive. It is generally acknowledged that acid compounds are easily oxidized by C–C activation to smaller molecule compounds. However, we observed that these acids, such as acrylic acid and acetic acid, are stable in the oxidation atmosphere over the $VOHPO_4{\cdot}0.5H_2O$ catalyst.

Based on the above results, we propose a simple reaction network starting from glycerol (Fig. 10). The dehydration of glycerol becomes more complex in the presence of oxygen, which possibly involves dehydration, oxidation, hydrogenation, and dehydrogenation reactions. When protonation occurs at the central hydroxyl group of glycerol, a water molecule and a proton are eliminated from the protonated glycerol, and then 3-hydroxypropanal is produced by tautomerism. In the actual reaction, 3-hydroxypropanal

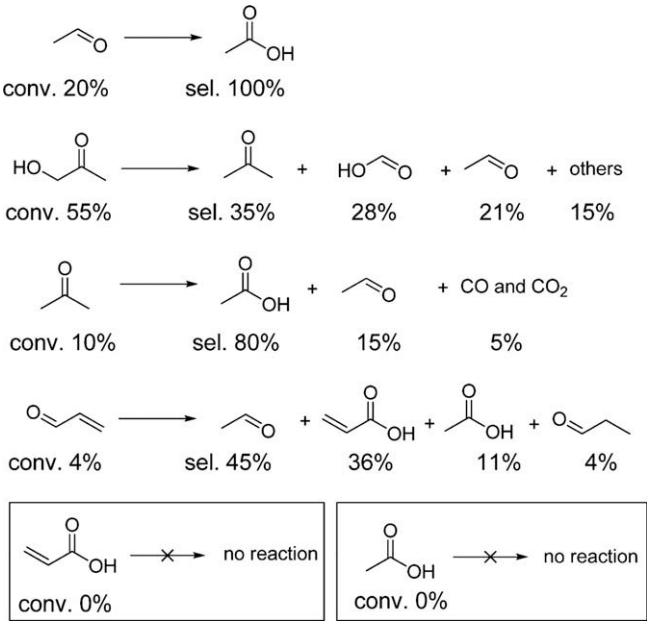

Fig. 9. Catalytic results using different substance over the $VOHPO_4{\cdot}0.5H_2O$ catalyst.

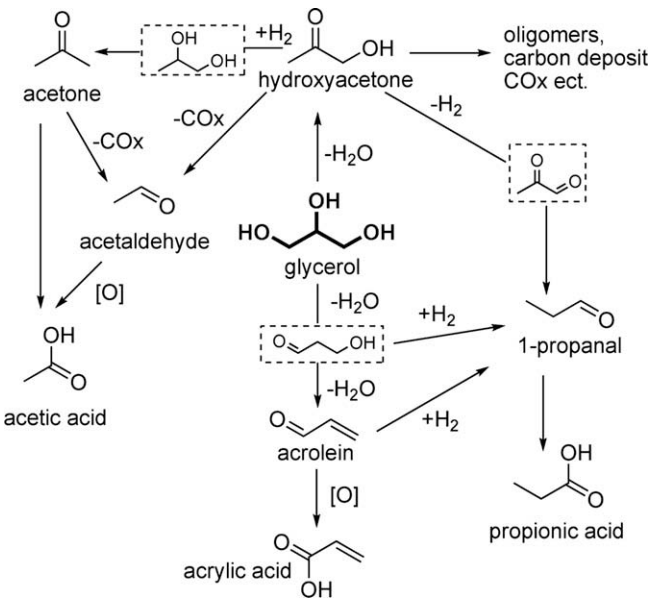

Fig. 10. Proposed general glycerol conversion scheme. The undetected products are shown by dashed rectangles.

is readily dehydrated into acrolein. In contrast, when protonation proceeds at a terminal hydroxyl group of glycerol, hydroxyacetone is produced through dehydration and deprotonation accompanied by tautomerism.

4. Conclusions

The performances of three VPO catalysts, $VOPO_4{\cdot}2H_2O$, $VOHPO_4{\cdot}0.5H_2O$, and $(VO)_2P_2O_7$, in the dehydration of glycerol in the presence of excess molecular oxygen were studied. The hemihydrate $VOHPO_4{\cdot}0.5H_2O$, which has never been known as an active catalyst, showed the best catalytic performance: 100% conversion of glycerol with 66% selectivity to acrolein and 14% selectivity to acetaldehyde. Both quantities and kinds of by-products were fewer than those in the literature works. The best carbon balance was achieved at 93%, which is much better than the literature results. GC–MS and TGA analyses indicated that there is no coke formation on the used catalyst when the reaction is conducted with an oxygen/glycerol ratio of 9.1. XRD, IR, and TGA characterizations revealed that the catalyst is stable during reaction. The reaction pathways were uncovered and this information will be helpful for further studies and as references. It has been shown that the $VOHPO_4{\cdot}0.5H_2O$ catalyst has limited ability for catalyzing the oxidation of acrolein to acrylic acid. In order to achieve the one-step conversion of glycerol to acrylic acid, a catalyst with greater oxidation ability and mild acidity is needed. Our future research will be focused on improving the oxidation ability of $VOHPO_4{\cdot}0.5H_2O$ by doping with other elements to achieve efficient conversion of glycerol to acrylic acid in one-step.

References

[1] A. Corma, S. Iborra, A. Velty, Chem. Rev. 107 (2007) 2411.
[2] Y. Zheng, X. Chen, Y. Shen, Chem. Rev. 108 (2008) 5253.
[3] C.-H. Zhou, J.N. Beltramini, Y.-X. Fan, G.Q. Lu, Chem. Soc. Rev. 37 (2008) 527.
[4] M. Aresta, A. Dibenedetto, F. Nocito, C. Pastore, J. Mol. Catal. A 257 (2006) 149.
[5] J.W. Yoo, Z. Mouloungui, Stud. Surf. Sci. Catal. 146 (2003) 757.
[6] G. Lewandowski, M. Bartkowiak, E. Milchert, Oxid. Commun. 31 (2008) 108.
[7] K. Murata, I. Takahara, M. Inaba, React. Kinet. Catal. Lett. 93 (2008) 59.
[8] E.P. Maris, R.J. Davis, J. Catal. 249 (2007) 328.
[9] T. Miyazawa, S. Koso, K. Kunimori, K. Tomishige, Appl. Catal. A 329 (2007) 30.
[10] S. Wang, H.C. Liu, Catal. Lett. 117 (2007) 62.
[11] Y. Fernandez, A. Arenillas, M.A. Diez, J.J. Pis, J.A. Menendez, J. Anal. Appl. Pyrol. 84 (2009) 145.
[12] S. Adhikari, S.D. Fernando, A. Haryanto, Chem. Eng. Technol. 32 (2009) 541.
[13] M. Bowker, P.R. Davies, L.S. Al-Mazroai, Catal. Lett. 128 (2009) 253.
[14] A. Karam, N. Villandier, M. Delample, C.K. Koerkamp, J.P. Douliez, R. Granet, P. Krausz, J. Barrault, F. Jerome, Chem. Eur. J. 14 (2008) 10196.
[15] A. Wolfson, C. Dlugy, Y. Shotland, Environ. Chem. Lett. 5 (2007) 67.
[16] S. Srivastava, V. Srivastava, V. Gupta, L. Chaudhary, Oxid. Commun. 30 (2007) 553.
[17] W.C. Ketchie, M. Murayama, R.J. Davis, Top. Catal. 44 (2007) 307.
[18] N. Dimitratos, A. Villa, C.L. Bianchi, L. Prati, M. Makkee, Appl. Catal. A 311 (2006) 185.
[19] E. Schwenk, M. Gehrke, F. Aichner, US Patent 1 916 743, Schering-Kahlbaum AG, 1933.
[20] A. Corma, G.W. Huber, L. Sauvanauda, P. O'Connor, J. Catal. 257 (2008) 163.
[21] S.H. Chai, H.P. Wang, Y. Liang, B.Q. Xu, Green Chem. 10 (2008) 1087.
[22] S.H. Chai, H.P. Wang, Y. Liang, B.Q. Xu, Appl. Catal. A 353 (2009) 213.
[23] S.H. Chai, H.P. Wang, Y. Liang, B.Q. Xu, J. Catal. 250 (2007) 342.
[24] E. Tsukuda, S. Sato, R. Takahashi, T. Sodesawa, Catal. Commun. 8 (2007) 1349.
[25] H. Atia, U. Armbruster, A. Martin, J. Catal. 258 (2008) 71.
[26] W. Yan, G.J. Suppes, Ind. Eng. Chem. Res. 48 (2009) 3279.
[27] Q.B. Liu, Z. Zhang, Y. Du, J. Li, X.G. Yang, Catal. Lett. 127 (2009) 419.
[28] L. Ott, M. Bicker, H. Vogel, Green Chem. 8 (2006) 214.
[29] M. Watanabe, T. Lida, Y. Aizawa, T.M. Aida, H. Inomata, Bioresour. Technol. 98 (2007) 1285.
[30] J.L. Dubois, C. Duquenne, W. Holderich, J. Kervennal, FR2882053 (A1), Arkema (FR), 2006.
[31] J.L. Dubois, C. Duquenne, W. Holderich, FR2882052, Arkema (FR), 2006.
[32] G.J. Hutchings, J. Mater. Chem. 19 (2009) 1222.
[33] G.S. Patience, R.E. Bockrath, J.D. Sullivan, H.S. Horowitz, Ind. Eng. Chem. Res. 46 (2007) 4374.
[34] G. Centi, J.L. Nieto, D. Pinelli, F. Trifiro, Ind. Eng. Chem. Res. 28 (1989) 400.
[35] V.V. Guliants, S.A. Holmes, J.B. Benziger, P. Heaney, D. Yates, I.E. Wachs, J. Mol. Catal. A 172 (2001) 265.
[36] N. Ballarini, F. Cavani, C. Cortelli, S. Ligi, F. Pierelli, F. Trifiro, C. Fumagalli, G. Mazzoni, T. Monti, Top. Catal. 38 (2006) 147.
[37] Q. Jiang, J. Zhao, X.X. Li, W.J. Ji, Z.B. Zhang, C.T. Au, Appl. Catal. A 341 (2008) 70.
[38] N. Yamamoto, N. Hiyoshi, T. Okuhara, Chem. Mater. 14 (2002) 3882.
[39] G. Koyano, T. Okuhara, M. Misono, J. Am. Chem. Soc. 120 (1998) 767.
[40] N. Mizuno, H. Hatayama, M. Misono, Chem. Mater. 9 (1997) 2697.
[41] C. R'Kha, M.T. Vandenborre, J. Livage, R. Prost, E. Huard, J. Solid State Chem. 63 (1986) 202.
[42] B.H. Sakakini, Y.H. Taufiq-Yap, K.C. Waugh, J. Catal. 189 (2000) 253.
[43] G.J. Hutchings, J. Mater. Chem. 14 (2004) 3385.
[44] S. Endres, P. Kampe, J. Kunert, A. Drochner, H. Vogel, Appl. Catal. A 325 (2007) 237.
[45] C. Schmitt, L. Giebeler, R. Schierholz, S. Endres, C. Fasel, H. Vogel, H. Fuess, Z. Phys. Chem. 221 (2007) 1525.
[46] J.L. Dubois, C. Duquenne, W. Holderich, FR2884817, Arkema (FR), 2006.
[47] J. Barrault, J.M. Clacens, Y. Pouilloux, Top. Catal. 27 (2004) 137.
[48] M.R. Nimlos, S.J. Blanksby, X.H. Qian, M.E. Himmel, D.K. Johnson, J. Phys. Chem. A 110 (2006) 6145.
[49] M. Ai, K. Ohdan, Bull. Chem. Soc. Jpn. 72 (1999) 2143.